JOURNAL OF MATERIALS SCIENCE 18 (1983) 2688–2696

Second phase development in Sr-doped TiO_2

H. C. LING
Engineering Research Center, Western Electric, Princeton, New Jersey 08540, USA
M. F. YAN
Bell Laboratories, Murray Hill, New Jersey 07974, USA

In the Ti-rich region of the SrO–TiO_2 system, a temperature–composition range is found to exhibit limited solubility of strontium, the maximum limit being 0.5 mol % Sr. It is also found that a two-phase region exists between this solubility limit and $SrTiO_3$, in agreement with existing phase diagrams. When the strontium concentration is small ($\leqslant$ 0.5 mol %), strontium segregates to the grain boundaries to form a second phase of $SrTiO_3$ below the solubility limit. Above 1200° C, this second phase is continuous; shape instability causes it to break up into discrete particles below 1200° C. At higher strontium concentration (about 2 mol % Sr), nucleation of $SrTiO_3$ crystallites occurs both inside the TiO_2 grains and at the grain boundaries. The morphology of these crystallites after long time annealing suggests that the {1 1 0} plane has the fastest growth rate. The appropriate range of composition and heat treatment to form a continuous $SrTiO_3$ grain boundary layer is discussed in relation to the optimum heat treatment to develop the best nonlinear electrical properties of varistor devices.

1. Introduction

In the system of BaO–TiO_2, several compounds are found in the compositional range between $BaTiO_3$ and TiO_2 [1–3]. Some of these compounds show desirable properties as dielectric materials. In sharp contrast, relatively few studies have been performed in the SrO–TiO_2 system. Published phase diagrams [4, 5] exhibit a two-phase region between $SrTiO_3$ and TiO_2 below the eutectic temperature of 1440° C. No intermediate compounds are indicated. In addition, relatively little is known about the solubility of SrO in TiO_2. This paper describes a study of the precipitation and identification of second phase(s) in strontium-doped TiO_2 materials.

2. Experimental details

Three TiO_2 compositions doped with 0.2, 0.5 and 2.0 mol % Sr were prepared. Fisher grade TiO_2 powder was thoroughly mixed with $Sr(NO_3)_2$ solution after which $(NH_4)_2CO_3$ was added to precipitate out strontium. The powder slurry was then spray-dried. In addition, one powder lot of $SrTiO_3$ was prepared by the usual solid-state reaction between TiO_2 and $SrCO_3$ to provide a standard in the scanning microscope (SEM) X-ray analysis. Approximately 0.6 g powder was pressed into discs of 6 mm diameter at 6.89×10^7 Nm^{-2} (10 000 psi). Some large discs of 25 mm diameter were also prepared as samples for X-ray diffraction analysis (XRD).

Unless otherwise specified, sintering in air took place initially at 1400° C for 2 h in order to establish a constant microstructure for a given composition. The heating rate was maintained at 400° Ch^{-1}. Samples were quenched into still air or cooled slowly at 50° Ch^{-1}. Some samples were annealed at intermediate temperatures between 1400 and 1150° C. In these cases, they were furnace quenched from 1400° C to the annealing temperature in less than three minutes. At the end of the annealing treatment, they were air quenched to room temperature in about 5 sec. The sintered samples have an average density of 4.9 g cm^{-3}, which is 95% of the theoretical density. Table I lists the heat treatment employed in this study.

Microstructures on the as-fired surfaces of the

0022–2461/83 $03.00 + .12

TABLE I Phases in Sr-doped TiO_2

Heat treatment conditions		Strontium composition		
Temperature (° C)	Time (h)	0.2 mol % Sr	0.5 mol % Sr	2.0 mol % Sr
1400	2 slow cool	discrete particles at GB	discrete particles at GB; transparent equiaxed particles	small particles at GB and interior of grains
1400	2 quenched	no second phase	continuous second phase at GB	small particles at GB and grain interior
	14 quenched	no second phase	continuous second phase at GB	substantial growth of some particles
1400	2 quenched to			
1350	18	no second phase	continuous second phase at GB	substantial growth of some particles
1300	18	no second phase	large transparent particles	substantial growth of some particles
1250	20	continuous second phase	continuous second phase at GB; large transparent particles	substantial growth of some particles
1200	24	discrete particles at GB	discrete particles at GB; large transparent particles	substantial growth of some particles
1150	24	discrete particles at GB	discrete particles at GB; large transparent particles	primarily small particles

GB–grain boundary.

ceramic discs were examined with optical and scanning electron microscopy. XRD and SEM X-ray analyses were used to identify the crystalline phases and their compositions, respectively.

3. Results

3.1. Slowly-cooled samples

Samples slowly-cooled from 1400° C show varying amounts of second phase on the surfaces. For TiO_2 with 0.2 mol % Sr, the second phases consist of small particles along the grain boundaries (Fig. 1a). When the strontium concentration is increased to 0.5 mol %, an additional morphology appears. Fig. 1b shows an equiaxed and transparent second phase grain, 20 μm in diameter, on top of the TiO_2 matrix. At 2 mol % Sr, many more small particles are found in the interior and at the boundaries of the matrix grains. To identify and to elucidate the formation of these second phases, samples were quenched from 1400° C to room temperature and to intermediate annealing temperatures between 1400 and 1150° C.

We had also examined the samples slowly-cooled after 2 h at 1450° C, ten degrees above the eutectic temperature. A second phase formation was observed as the result of slow cooling. Furthermore, the grain size has increased to 50 to 100 μm. The intergranular area in the 0.5 mol % Sr composition is quite large and it indicates the presence of a liquid phase at 1450° C (Fig. 2a). This is consistent with the published phase diagrams. However, the 0.2 mol % Sr composition, Fig. 2b, exhibits no evidence of liquid phase formation. The grain boundary is broader than the 1400° C sintering, due to thermal etching effects.

3.2. Samples quenched from 1400° C

After two hours at 1400° C, the quenched TiO_2 samples with 0.2 and 0.5 mol % Sr do not show the discrete second phases seen in the slowly cooled samples. Under high magnification, there appears to be outgrowth at some grain boundaries in the 0.5 mol % Sr samples (Fig. 3a). This is shown more clearly in the SEM micrograph (Fig. 3b), where the grain boundary is covered by a continuous second phase, which has wavy boundaries. SEM X-ray analysis shows substantial strontium segregation to the grain boundary as compared to the matrix where only titanium is detected (Fig. 3c). There is no oxygen peak because oxygen excitation lies below the detection limit of the instrument. The ratio of the strontium to titanium peak intensities is similar to that

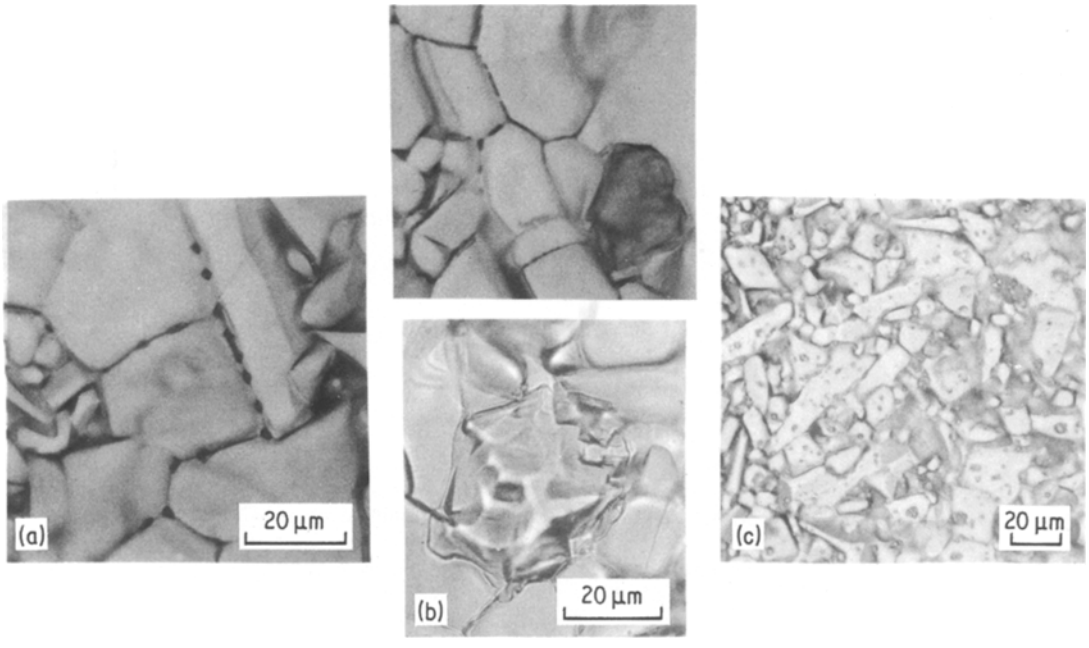

Figure 1 Optical micrographs of (a) 0.2 mol % Sr, (b) 0.5 mol % Sr and (c) 2.0 mol % Sr samples slow-cooled after 2 h at 1400° C.

of the $SrTiO_3$ standard. A small calcium peak is also present in the boundary phase. In contrast, strontium segregation is not apparent in the 0.2 mol % composition. This is indicated by strontium mapping and X-ray analysis of a triple junction (Figs. 3e and f). Thus, up to 0.2 mol % Sr is in solution with TiO_2 at 1400° C. SEM X-ray analysis of the matrix revealed no strontium due to the small concentration. The 2 mol % Sr composition has a microstructure similar to the slowly cooled samples.

To ensure that an equilibrium microstructure is observed, some samples were annealed for 14 h at 1400° C. They have essentially the same microstructure. There is some growth of the second phase in the 2 mol % composition. Similar growth is seen in samples annealed at the lower temperatures. This will be discussed in the next section.

3.3. Annealed samples

Table I summarizes the appearance of second phases as a function of annealing temperature. In the 0.2 mol % Sr composition, strontium

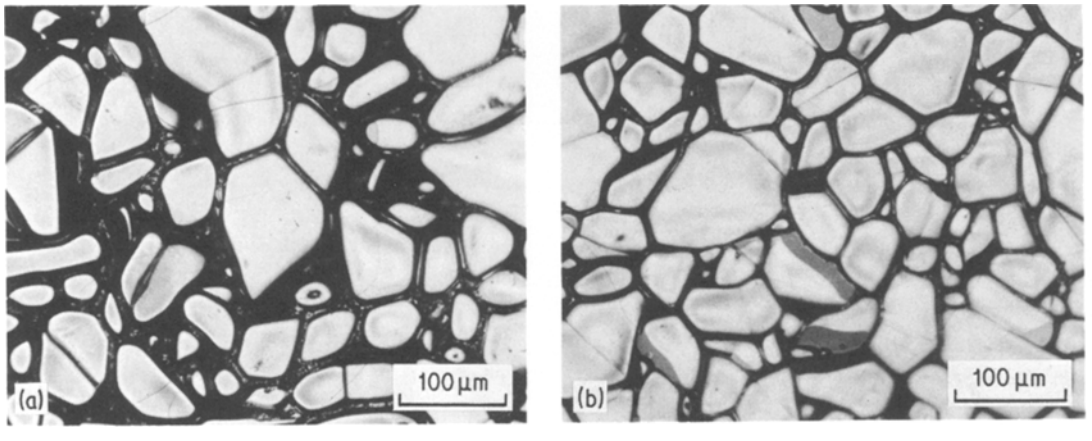

Figure 2 Optical micrograph of (a) 0.5 mol % Sr and (b) 0.2 mol % Sr samples slow-cooled after 2 h at 1450° C.

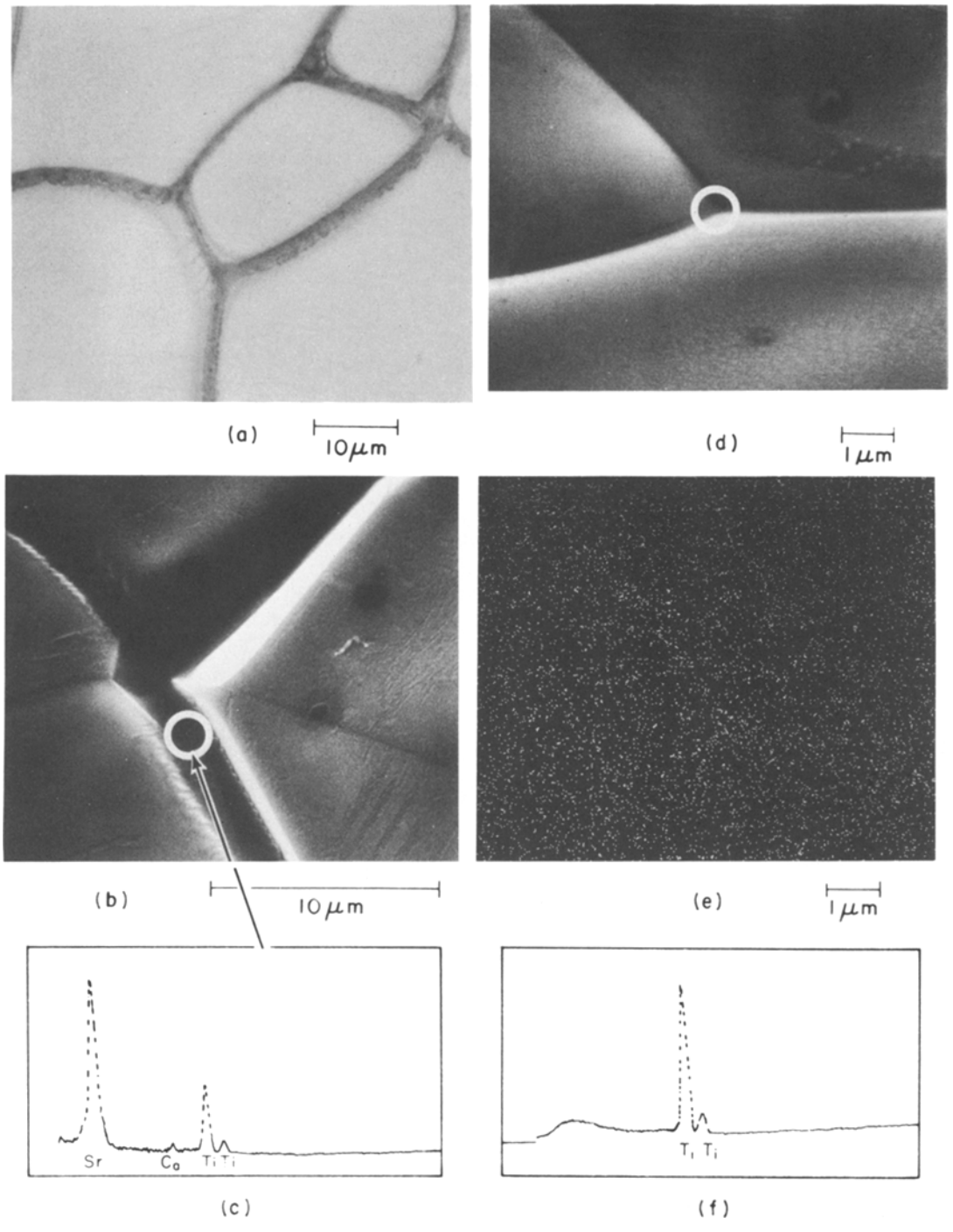

Figure 3 Segregation to grain boundaries in samples quenched after 2 h at 1400° C: (a) 0.5 mol% Sr, optical micrograph; (b) 0.5 mol% Sr, SEM; and (c) the associated X-ray analysis; (d) 0.2 mol% Sr, SEM; (e) strontium mapping of the same area with (f) the X-ray analysis of the triple junction.

segregation was not detected at temperatures $\geqslant$ 1300° C (Fig. 4a). At 1200° C, however, elongated second phase particles are definitely present along the grain boundaries (Fig. 4b). The distribution is rather nonuniform, as illustrated by the SEM micrograph in Fig. 4c. In general, most of these second phase particles are strontium rich and the Sr/Ti peak intensity ratio is similar to that of

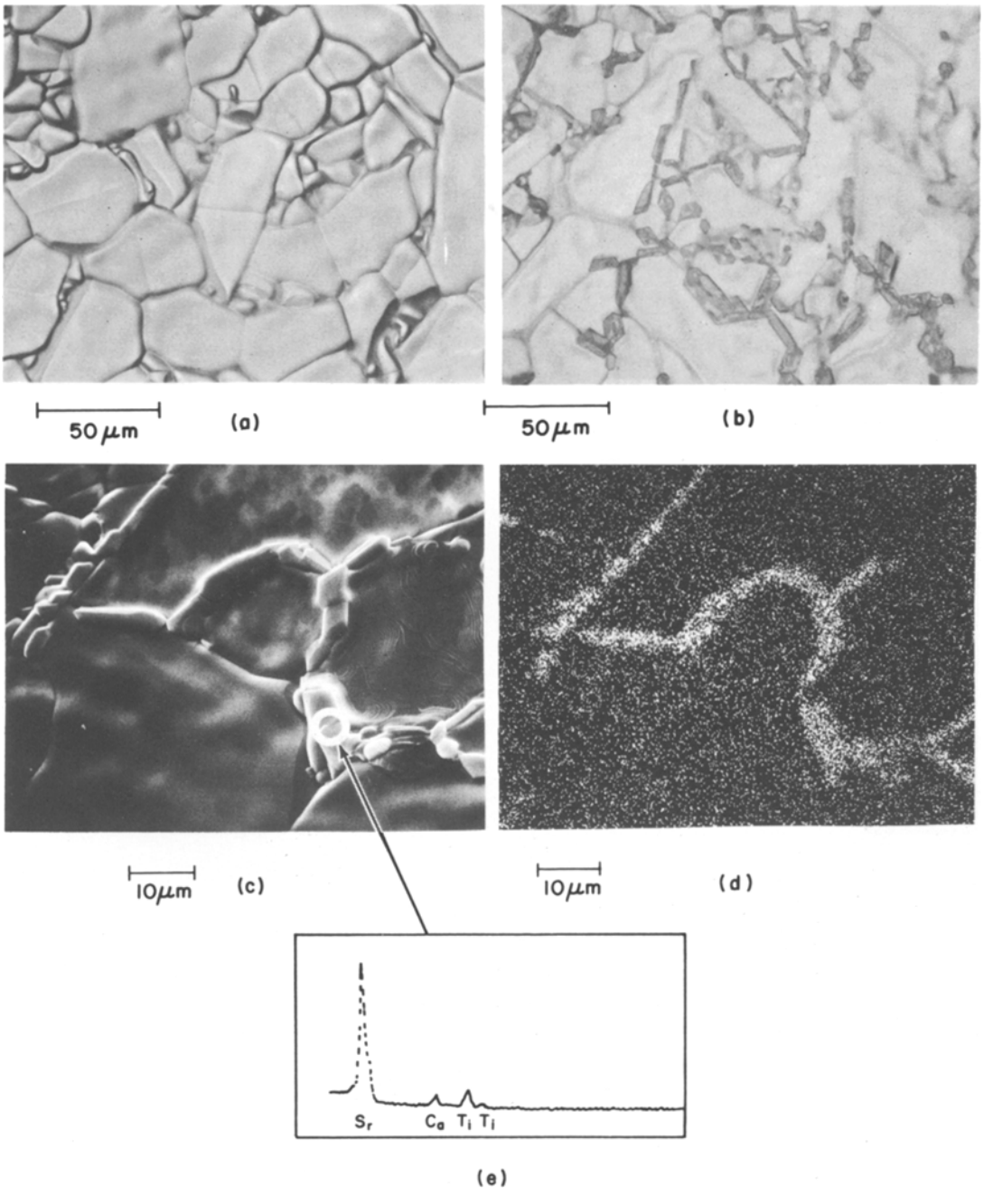

Figure 4 Precipitation of second phase in 0.2 mol % Sr composition after quenching from 1400° C (2 h) to and annealed at (a) 1250° C 20 h; (b) 1200° C 24 h optical micrograph; (c) 1200° C 24 h SEM and (d) strontium mapping of the same area in (c); SEM X-ray analysis of circled area in Fig. 4c is shown in Fig. 4e.

$SrTiO_3$. XRD of large disc specimens also shows only $SrTiO_3$ peaks in addition to the rutile pattern. However, in certain local areas calcium segregation is more prominent and the titanium concentration is less rich (Fig. 4e); then the local composition is different from $SrTiO_3$. This is probably due to an inhomogeneous mixing of the dopant in ceramics.

In the 0.5 mol % Sr composition, large equiaxed and transparent particles appear below 1300° C. Fig. 5a shows a SEM micrograph of such a particle as a thin layer on top of the rutile (TiO_2) matrix. It is strontium rich and the Sr/Ti X-ray intensity ratio is the same as $SrTiO_3$. In addition, strontium segregates to form a continuous second phase at

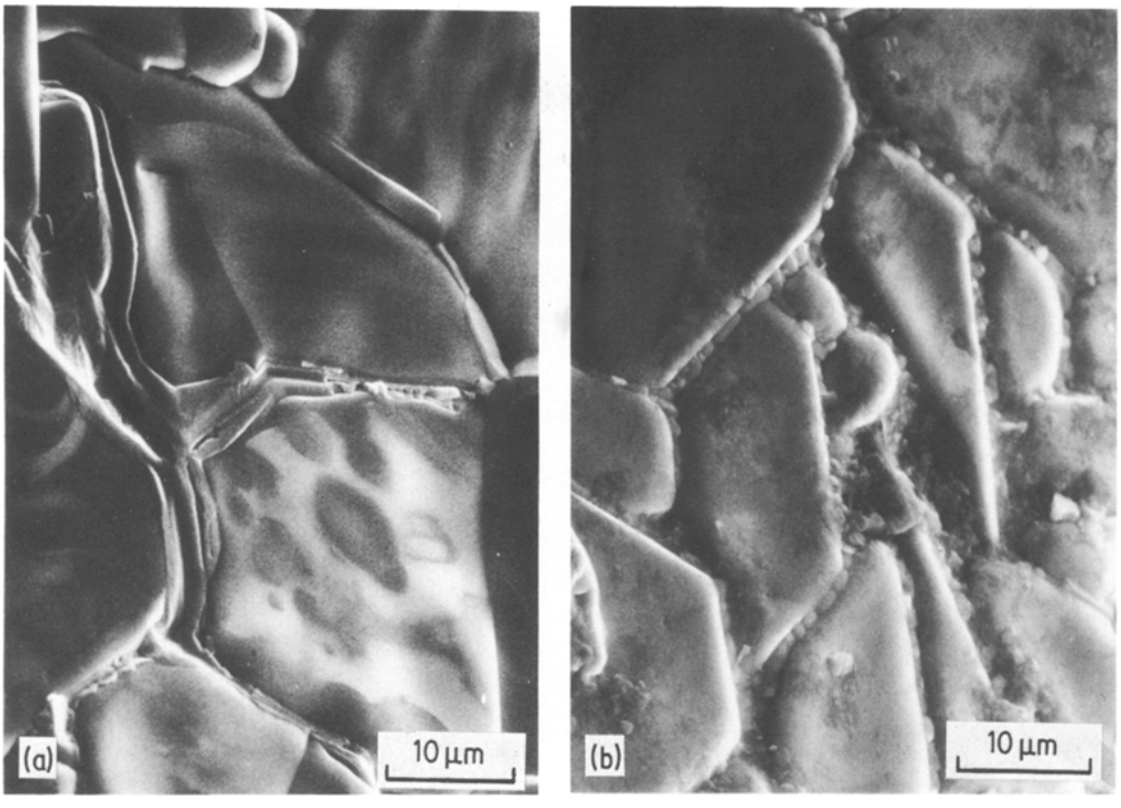

Figure 5 Different second phase morphologies in 0.5 mol % Sr composition: (a) large, transparent particles, 1400° C 2 h and annealed at 1200° C 24 h (b) discrete, GB particles, 1400° C 2 h quenched to room temperature followed by 1200° C 2 h and (c) continuous GB second phase, 1400° C 2 h and annealed at 1250° C 20 h; all SEM micrographs.

the grain boundaries between 1400 and 1250° C. Below 1200° C, the grain boundaries are lined with discrete particles instead. To show that the two morphologies of second phase at the grain boundary are related, samples quenched from 1400° C were reannealed at 1200° C for 2 h. Indeed, the original continuous layer has broken up into discrete particles. Figs. 5b and c give a comparison between this morphology and a continuous grain boundary layer in a sample annealed at 1250° C for 20 h. Again, only $SrTiO_3$ peaks are detected in XRD in addition to the rutile pattern, indicating that only $SrTiO_3$ is formed as a second phase in this composition.

In the 2 mol % Sr composition, some of the second phase particles exhibit substantial growth during the annealing treatment. The growth rate decreases with lowering annealing temperature;

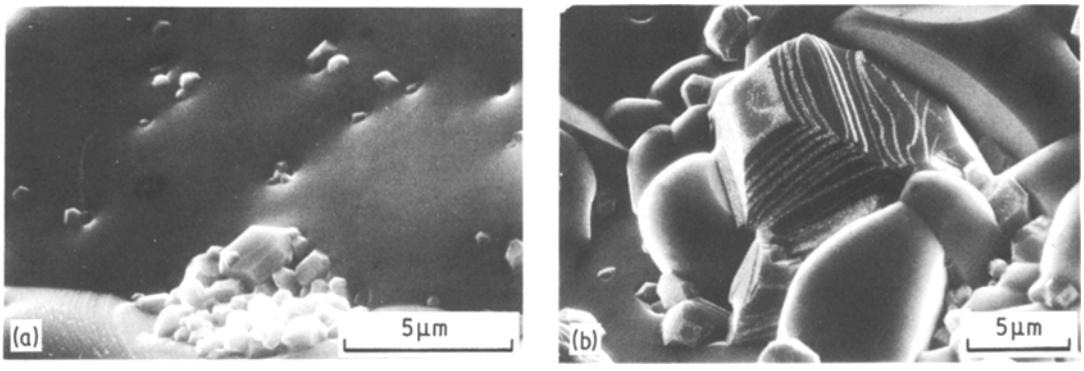

Figure 6 $SrTiO_3$ crystallites in 2.0 mol % Sr composition: (a) 1400° C 2 h quenched and (b) further annealed at 1300° C 18 h.

at 1150° C, the microstructure is similar to that quenched after 2 h at 1400° C as shown in Fig. 6a. The particle morphology changes during the growth process. The small particles consist of a mixture of hexagonal, rectangular and square faces (Fig. 6a). As growth proceeds, the (110) plane becomes the dominant feature so that after long time annealing, the large particles are pyramid-like structures with the rectangular top protruding from the TiO_2 matrix as shown in Fig. 6b. They show the same Sr/Ti intensity ratio as $SrTiO_3$. XRD analysis also indicates that only TiO_2 rutile and $SrTiO_3$ phases are present in the sample. Fig. 7 summarizes the occurrence of second phase morphology at the different temperature investigated in this study.

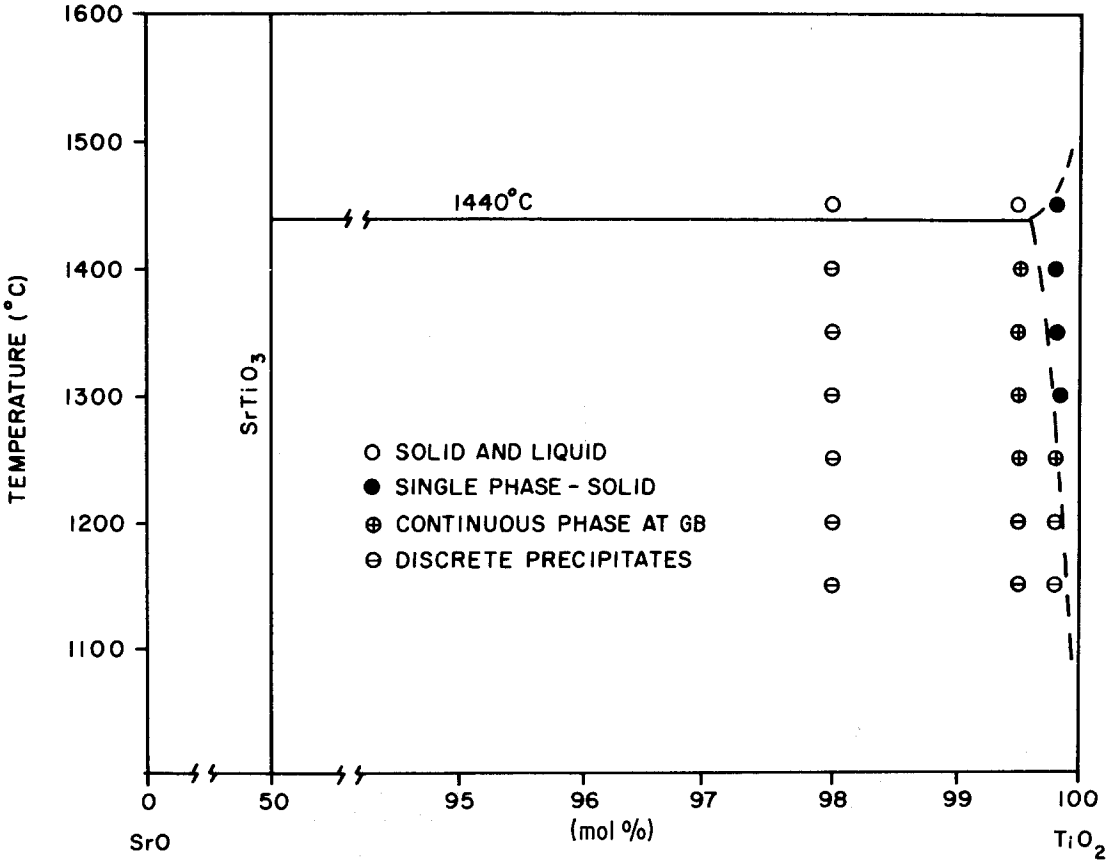

Figure 7 Proposed SrO–TiO_2 phase diagram in the TiO_2-rich region.

4. Discussion

Investigation of three Sr-doped TiO_2 compositions shows that $SrTiO_3$ is the only second phase formed between 1400 and 1150° C. This confirms the existing $SrTiO_3$–TiO_2 phase diagram that there exists no other intermediate compound in the compositional range between $SrTiO_3$ and TiO_2 below the eutectic temperature of 1440° C. In addition, up to 0.2 mol% Sr is found to be soluble in TiO_2 between 1400 and 1300° C. Precipitation of $SrTiO_3$ as a second phase probably begins between 1250 and 1200° C at the 0.2 mol% Sr composition. Furthermore, we do not observe any liquid phase formation at this composition at 1450° C. As a result, the phase diagram should show a line of solubility limit of SrO in TiO_2, as indicated by the dashed curve in Fig. 7. The melting point of TiO_2 is at 1840° C.

One major driving force for solute segregation is the size misfit between the solute and matrix ions. Their segregation to the grain boundaries or free surfaces provides a partial relaxation of the elastic strain energy [7]. Eshelby [8] showed that the misfit energy is proportional to the square of the size misfit, Δr. With an ionic radius of 0.113 nm, the size misfit due to strontium substitution in the titanium site ($r = 0.068$ nm) is smaller than that of a barium substitution ($r = 0.135$ nm). The elastic misfit energy associated with the strontium solute is 226 kJ mol^{-1} (54 kcal mol^{-1}) at 1200° C, less than half of the value of 502 kJ mol^{-1} (120 kcal mol^{-1}) calculated for a barium solute [6]. Thus it is perhaps not surprising to find some strontium solubility in the rutile matrix above 1300° C. It is also obvious that barium will segregate more readily to the grain boundaries and serve as a more efficient misfit dopant.

At the 0.5 mol% Sr composition, strontium segregates to the grain boundaries to form a continuous second phase between 1400 and 1250° C. It has wavy boundaries with a periodicity (wavelength) smaller than its width at 1400° C (Fig. 3b). Below 1200° C, this continuous second phase breaks up into discrete precipitates with a length generally several times its width. This morphological transition suggests an instability similar to the breakdown of a liquid cylinder into a row of spherical droplets, first discussed by Lord Rayleigh [9]. Cline [10] performed a similar analysis on the high temperature stability of a system of solid cylindrical rods in a composite geometry. Variation in the shape of the rods was assumed to result in diffusive transport through the matrix under the driving force of capillarity. The analysis showed that a cylindrical geometry is stable with respect to perturbations with wavelengths smaller than the circumference of the unperturbed rod because of increased total interface energy. This appears to be the case at 1400° C in the Sr-doped TiO_2 samples. At the lower annealing temperatures, further precipitation of $SrTiO_3$ may have changed the shape perturbation so that some components of the wavelength factor exceed the minimum criterion and will grow. The theoretical analysis predicts a maximum rate of growth of the perturbation at a wavelength of 14 R_0 where R_0 is the radius of the unperturbed rod. This suggests that when the cylindrical rod breaks up into discrete particles, they have a length to width (aspect) ratio predominantly about 7. The aspect ratio of the discrete precipitates observed in the Sr-doped TiO_2 samples varies over a wide range, with the value of seven probably as the upper limit. Since it is unlikely that the continuous $SrTiO_3$ second phase assumes an idealized cylindrical shape in the first place, its disintegration into discrete precipitates can reasonably be attributed to shape instability at elevated temperatures, as described by Cline's theory [10].

At the 2 mol% Sr composition, the greater strontium concentration causes the nucleation of many $SrTiO_3$ precipitates in the interior of the TiO_2 grains in addition to the formation at the grain boundaries. These small crystallites of $SrTiO_3$ adopt a geometrical shape which illustrates the principle of minimum total surface energy for a fixed amount of matter. Sundquist [11] considered different bond energies to both the first and second nearest neighbours and calculated the surface free energy as a function of orientation. For the fcc structure, the close-packed {111} planes have the lowest energy and for the bcc structure, the {110} planes have the lowest energy. In the $SrTiO_3$ perovskite structure, the cations form the bcc structure with the oxygen anions occupying the face-centred positions. The Wulff construction [12] of a polar surface energy γ-plot will give a mixture of {111}, {110} and {100} plane as the equilibrium crystal shape. These are the hexagonal, rectangular and square facets observed in the $SrTiO_3$ crystallites (Fig. 6a) and the corners and edges are sharp. Compara-

tively, the equilibrium shape of small fcc nickel particles [11] is also faceted with {111} and {100} faces, but the edges and corners are rounded. The difference in sharpness of the edges and corners indicates that the cusps in the γ-plot is sharper in $SrTiO_3$. In other words, a slight misorientation from the low-indexed planes will increase the surface energy rapidly.

As crystallites increase in size, it is much more common for their shape to be the result of the way in which they grew. The growth of these $SrTiO_3$ crystallites to pyramid-like structures, Fig. 6b, approximately 10 μm in height, appears to be a result of rapid accumulation of {110} planes. It is likely that at even longer annealing times, the pyramid structure will become pointed, as the {110} planes outgrow the other crystallographic planes. This suggests that the {110} planes may have a faster growth rate than the other orientations. When the growth rate of a crystal is determined only by the rate at which its surfaces can accept atoms, then the rate of advance of a surface will depend only on its crystallographic orientation. This is true for a cubic crystal such as $SrTiO_3$, since material transport in this lattice is isotropic. Computer simulation of fcc crystal growth [13], taking into account only the nearest neighbour interaction, concluded that the {110} plane has the fastest growth rate, followed by {100} and {111} planes. The observed growth of $SrTiO_3$ crystallites is in qualitative agreement with this analysis.

In certain device applications, e.g. varistors and grain boundary capacitors, it is desirable to have a continuous layer of second phase along the grain boundaries [14]. This study has shown the compositional range and temperature treatment for the Sr-doped TiO_2 system to ensure the formation of a continuous grain boundary phase. The composition should be greater than 0.2 mol% Sr, but not more than 0.5 mol% to avoid intragranular nucleation. The boundary layer thickness will be larger for a larger strontium composition. Once this layer is formed, extensive period of exposure to temperatures below 1250° C should be avoided in order to prevent disintegration of the continuous layer into discrete particles. Thus an optimum heat treatment will be sintering at 1400° C, followed by slow cooling between 1400 and 1300° C to allow sufficient time for strontium segregation to the grain boundaries and rapid cooling below 1300° C. This is consistent with the optimal heat treatments to give the maximum non-linearity index in TiO_2 varistors [15].

Acknowledgements

We thank W. W. Rhodes of BTL-MH for powder and sample preparations and R. Woods of WE-ERC for SEM work.

References

1. D. E. RASE and R. ROY, *J. Amer. Ceram. Soc.* **38** (1955) 102.
2. H. M. O'BRYAN and J. THOMPSON Jr, *ibid.* **57** (1974) 522.
3. R. K. SHARMA, N. H. CHAN and D. M. SMYTH, *ibid.* **64** (1981) 448.
4. R. ROY (1957), cited in "Phase Diagrams for Ceramists", edited by E. M. Levin, C. R. Robbins and H. F. McMurdie (The American Ceramic Society, Columbus, Ohio, 1969).
5. A. COCCO and F. MASSAZZA, *Ann. Chim. (Rome)* **53** (1963) 892, as cited in "Phase Digrams for Ceramists", edited by E. M. Levin, C. R. Robbins and H. F. McMurdie (The American Ceramic Society, Columbus, Ohio, 1969).
6. H. M. O'BRYAN and M. F. YAN, *J. Amer. Ceram. Soc.* **65** (1982) 615.
7. M. F. YAN, R. M. CANNON and H. K. BOWEN, in "Grain Boundaries in Semiconductors", edited by H. J. Leamy, G. E. Pike and C. H. Seager, (Elsevier Science Publishing, New York, 1982) pp. 57–62.
8. J. D. ESHELBY, *Prog. Solid Mech.* **2** (1961) 99.
9. LORD RAYLEIGH, *Lond. Math. Soc. Proc.* **10** (1879) 4.
10. H. E. CLINE, *Acta Metall.* **19** (1971) 481.
11. B. E. SUNDQUIST, *ibid.* **12** (1964) 67.
12. J. W. CHRISTIAN, "The Theory of Transformations in Metals and Alloys" (Pergamon Press, Oxford, 1965).
13. G. M. GILMER and K. A. JACKSON, in "Current Topics in Materials Science" Vol. 2, edited by E. Kaldis and H. J. Scheel (North-Holland, Amsterdam, 1976).
14. M. F. YAN and W. W. RHODE, *Appl. Phys. Lett.* **40** (1982) 536.
15. M. F. YAN and W. W. RHODES, Proceedings of Materials Research Society, Boston, edited by H. J. Leamy, G. E. Pike and C. H. Seager, (Elsevier Science Publishing, New York, 1982) pp. 357–62.

Received 4 January
and accepted 20 January 1983